Ratiometric temperature sensing with fluorescent thermochromic switches

(Article begins on next page)

10 April 2024

Ratiometric temperature sensing with fluorescent thermochromic switches

Mercedes M. A. Mazza[a], Francesca Cardano[abc], Janet Cusido[ad], James D. Baker[a], Silvia Giordani[bef] and Françisco M. Raymo*[a]

[a]*Laboratory for Molecular Photonics, Departments of Biology and Chemistry, University of Miami, Coral Gables, USA. E-mail: fraymo@miami.edu*

[b]*Nano Carbon Materials, Istituto Italiano di Tecnologia, Turin, Italy*

[c]*Department of Chemistry and Industrial Chemistry, University of Genoa, Genoa, Italy*

[d]*Department of Natural and Social Sciences, Miami Dade College – InterAmerican Campus, Miami, USA*

[e]*Department of Chemistry, University of Turin, Torino, Italy*

[f]*School of Chemical Sciences, Dublin City University, Glasnevin, Ireland*

Abstract

The connection of fluorescent chromophores to switchable heterocycles translates into molecular probes with ratiometric response to temperature. The opening and closing of their heterocyclic component equilibrates two emissive species with resolved fluorescence. Their relative emission intensities change monotonically with temperature to enable the visualization of thermal distributions at the microscale.

The ability to measure temperature with spatial resolution at the sub-micrometer level is crucial for the fundamental understanding of diverse cellular processes[1–3] and can have profound technological implications.[4,5] The requirement of physical contact between sample and sensor, however, prevents the miniaturization of conventional thermometry to

this dimensional scale. These limitations are stimulating the development of alternative thermometric methods based on optical measurements.[6] In this context, the noninvasive character, ultrahigh sensitivity and fast response times of fluorescence, together with the inherent temperature dependence of the excitation dynamics of organic chromophores, are particularly convenient.[7] Indeed, remarkable examples of molecular and macromolecular systems capable of responding to temperature with fluorescence changes have been reported already.[8–12] In most instances, temperature affects the rates of the radiative and nonradiative deactivation of these chemical thermometers and, as a result, alters the intensity of their emission bands. Nonetheless, concentration effects and optical artifacts can influence significantly intensity measurements at a single wavelength.[13–15] In order to overcome these complications, distinct organic chromophores with resolved emission bands can be paired within thermosensitive macromolecular or supramolecular constructs to ensure ratiometric temperature response.[16–20] Temperature-induced geometrical changes of the scaffold holding the two components together generally affect their excitation dynamics and their relative emission intensities. Structural designs to engineer thermosensitive dual emission from a single chromophore could be a valuable alternative to these established methods. Indeed, they could provide the opportunity to avoid the relatively large dimensions of macromolecular backbones or supramolecular containers to enable the implementation of molecular-sized thermometers with ratiometric response.

Thermochromic compounds alter reversibly their ability to absorb visible light in response to temperature.[21] Generally, the interconversion of two isomers with resolved absorption bands is responsible for these effects. In principle, the two interconverting species could be engineered also to emit in distinct spectral regions. Under these conditions, a change in temperature would alter the relative intensities of the two resolved emissions and offer the opportunity to perform ratiometric measurements. These

considerations suggested the possibility to explore the influence of temperature on the opening and closing of oxazine heterocycles. Indeed, our laboratories developed already halochromic and photochromic fluorophores based these reversible transformations.[22–24] Presumably, their structural design can be adapted to impose thermal response with dual fluorescence.

The ring-closed and -open isomers of 1 (Cl and Op in Fig. 1) interconvert with fast kinetics in acetonitrile at ambient temperature.[25] In particular, variable temperature ^{1}H NMR spectroscopy and time-resolved absorption spectroscopy indicate the rate constants for ring-opening and -closing to be 7×10^2 and 5×10^{-6} s^{-1} respectively at 298 K. The coumarin chromophores of the two isomers emit in resolved spectral windows.[26] Specifically, the emission maximum shifts bathochromically by *ca.* 200 nm with the opening of the 2*H*,4*H*-benzo[1,3]oxazine (oxazine) heterocycle. Indeed, only then can the coumarin chromophore extend its electronic conjugation over the resulting indolium cation. In principle, the ratio between the intensities of the two resolved emissions should change with temperature, if this physical parameter can affect the equilibrium between the two isomers. Should this be the case, then the spontaneous opening and closing of oxazine heterocycles might become a viable mechanism to design fluorescence sensors capable of responding ratiometrically to temperature. These considerations suggested the investigation of the temperature dependence of the equilibria between the ring-closed and -open isomers of four related molecular switches (1–4 in Fig. 1). Compound 3Cl incorporates a carbazole chromophore, in place of the coumarin component of 1Cl, and was synthesized according to a literature procedure from our laboratories.[27] Compounds 2Cl and 4Cl have a 2*H*,3*H*,4*H*,5*H*-[1,3]oxazole (oxazolidine) heterocycle, instead of the oxazine ring of 1Cl and 3Cl, and were prepared in a single step from known precursors (Fig. S1, ESI).
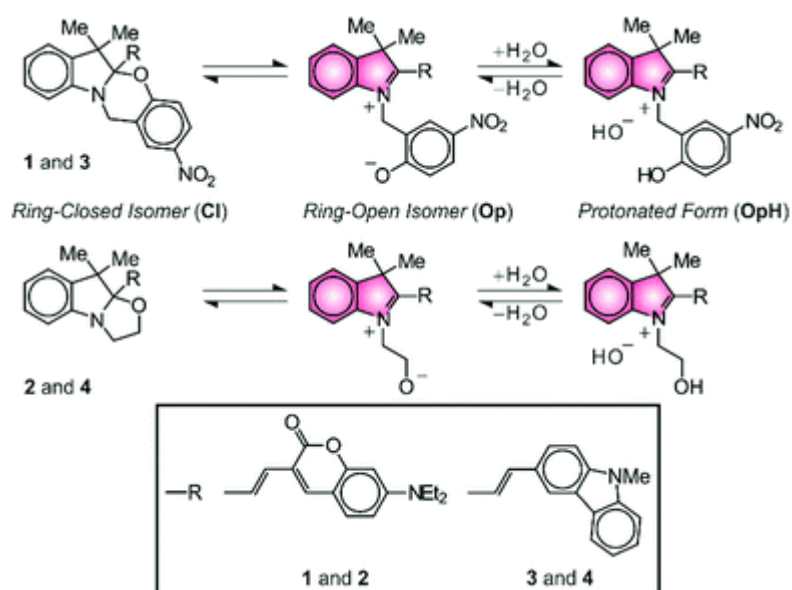
Fig. 1 Interconversion of the ring-closed (Cl) and -open (Op) isomers of 1–4 and their protonated forms (OpH).

The absorption spectra (Fig. 2) of 1–4 in acetonitrile at micromolar concentrations show the characteristic bands of the coumarin and carbazole chromophores associated with the ring-closed isomers. Specifically, the wavelength (λ_{Ab}) of the absorption maximum for the coumarin component of 1Cl and 2Cl is 412 nm.[25] Those for the pair of bands corresponding to the carbazole chromophore of 3Cl and 4Cl are 240 and 287 nm.[27] Comparison to the absorption spectra of appropriate model compounds (8 and 9 in Fig. S3, ESI) indicates that the carbazole absorptions partially overlap those associated with the indole and 4-nitrophenoxy fragments.
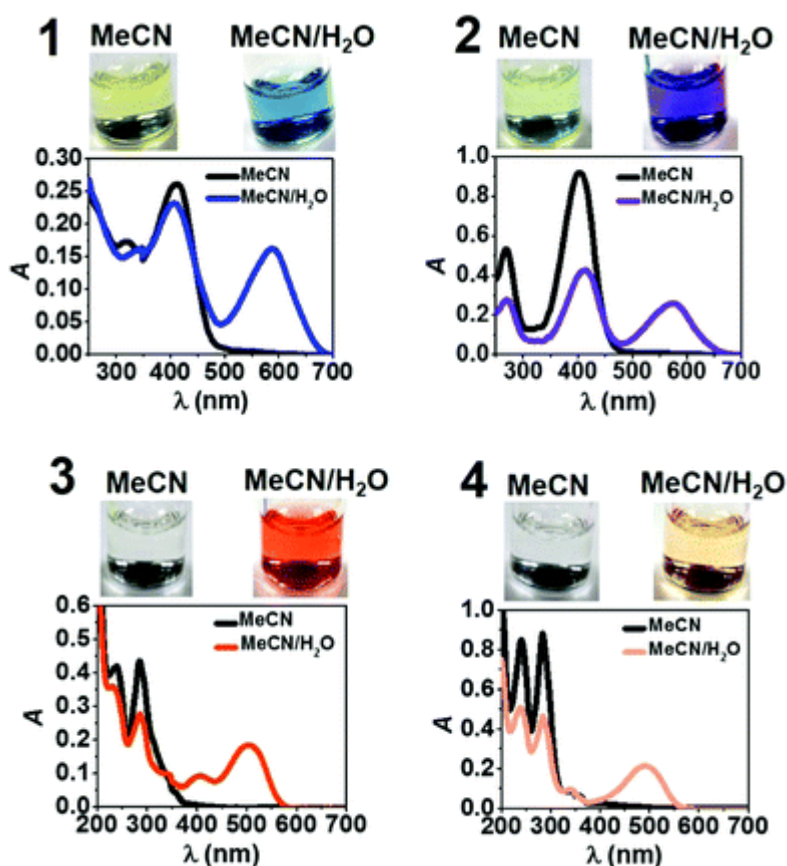
Fig. 2 Absorption spectra of 1–4 (15–120 μM) in MeCN and MeCN/H₂O (1 : 1 v/v) at 293 K and photos of the corresponding solutions.

The absorption spectra of model compounds (10 and 11 in Fig. S3, ESI) with extended chromophoric platforms analogous to those of 1Op–4Op suggest that the coumarin and carbazole fragments of the ring-open isomers should absorb in the visible region. Indeed, bands in this spectral window can be detected when either the total concentration of the pair of interconverting isomers is raised to the millimolar level (Fig. S4, ESI) or in the presence of water (Fig. 2). These observations indicate that the ring-closed isomer is significantly more stable than the ring-open one in acetonitrile for all systems and that water facilitates ring opening. The latter effect can be a consequence of the increase in solvent polarity with a concomitant stabilization of 1Op–4Op and/or their protonation to form 1OpH–4OpH. Density functional theory[29] (DFT) calculations, performed on model compound 8 (Fig. S12 and S13) with solvation models for either acetonitrile or water,

suggest that the change in the dielectric constant of the medium has a negligible influence on the relative energies of the two isomers.

Instead, the pK_a values reported in the literature[31] for 4-nitrophenol (7.15) and ethanol (15.50) imply that the protonation of the ring-open isomer is essentially quantitative in the presence of water. Thus, the absorption bands observed at long wavelengths in a mixture of acetonitrile and water can be assigned to the extended chromophores of 1OpH–4OpH.

The absorption spectra (<u>Fig. 3</u> and Fig. S5–S7, ESI) of 1–4 in a mixture of acetonitrile and water display significant temperature dependence. In all instances, the absorbance of the ring-closed isomer at short wavelengths increases and that of the protonated form at long wavelengths decreases with a raise in temperature. From the absorbance values at the maxima of these bands, the concentrations of 1Cl–4Cl and 1OpH–4OpH can be estimated at each temperature (T) to quantify the corresponding equilibrium constants (K_{Eq}). In turn, the enthalpic (ΔH) and entropic ($T\Delta S$) terms governing these equilibria can be evaluated from the slope and intercept respectively of logarithmic plots (Fig. S8,) of K_{Eq} against the inverse of temperature. The resulting values are listed in Table S1. In all instances, $T\Delta S$ is significantly more negative that ΔH in agreement with the pronounced temperature dependence of the absorption spectra. Interestingly, the ΔH values of the oxazolidine derivatives (2 and 4) are more negative than those of the oxazine counterparts (1 and 3), consistently with the large pK_a difference between their protic functional groups. Similarly, the $T\Delta S$ values of the carbazole derivatives (3 and 4) are more negative than those of the coumarin counterparts (1 and 2), perhaps as a result of solvation effects and/or the conformational freedom associated with the diethylamino substituent of the latter.
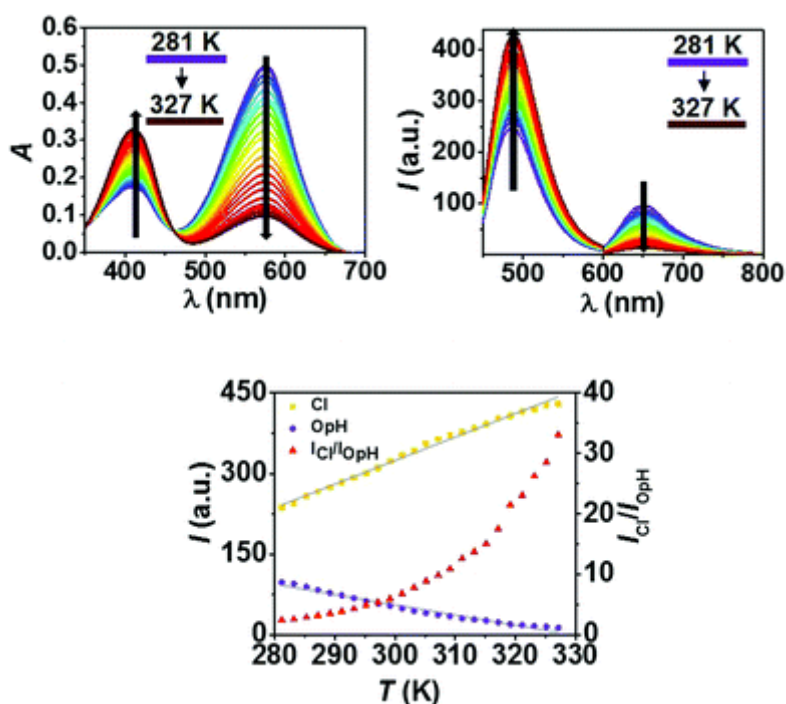
Fig. 3 Absorption (left) and emission (right, λ_{Ex} = 415 and 575 nm) spectra of 2 (24 μM) in MeCN/H$_2$O (1 : 1 v/v) at temperatures ranging from 281 to 327 K together with the temperature dependence (bottom) of the emission intensities of Cl and OpH and their ratio.

In a mixture of acetonitrile and water, the coumarin chromophores of ring-closed isomers 1Cl and 2Cl absorb at a λ_{Ab} of 412 nm (Table S1) and produce fluorescence with emission maxima at wavelengths (λ_{Em}) of 475 and 489 nm respectively. However, the fluorescence quantum yield (ϕ) of 1Cl is only 0.01, while that of 2Cl is 0.98. Such a pronounced difference in ϕ indicates that the presence of a 4-nitrophenoxy fragment in 1Cl must encourage the nonradiative deactivation of the excited coumarin fluorophore. A similar effect is observed also for protonated forms 1OpH and 2OpH. They emit at λ_{Em} of 650 and 660 nm with ϕ of 0.02 and 0.15 respectively. Once again, the presence of a 4-nitrophenol fragment in 1OpH is promoting the nonradiative deactivation of the excited fluorophore. Presumably, the electron deficient nitro groups of 1Cl and 1OpH can accept an electron from the corresponding coumarin chromophores upon excitation in both instances to quench fluorescence.

Under the same experimental conditions, the carbazole chromophores of ring-closed isomers 3Cl and 4Cl absorb at λ_{Ab} of 240 and 287 nm (Table S1) However, only 4Cl produces fluorescence at λ_{Em} of 371 and 383 nm with ϕ of 0.18. The 4-nitrophenoxy fragment of 3Cl must be responsible for suppressing the ability of the carbazole chromophore to emit. Indeed, literature data[27] from our laboratories suggest that the photoinduced transfer of one electron from the latter component to the former is exergonic with a free-energy change of −0.7 eV. Once again, a similar effect is observed also for protonated forms 3OpH and 4OpH. The extended electronic conjugation of their chromophoric platforms shifts λ_{Ab} to the visible region, but only the latter compound produces fluorescence at a λ_{Em} of 596 nm with ϕ of 0.02.

The significant temperature dependence of the equilibrium between the ring-closed isomer and protonated form of 1–4, obvious from the absorption spectra, translates into a ratiometric fluorescence response. Indeed, the relative intensities of the emission bands of the two equilibrating species change with temperature (Fig. 3 and Fig. S5–S7) apart from 3, which is essentially not emissive. This effect is especially evident for 2Cl and 2OpH, because their ϕ values are significantly larger than those of the other systems. Specifically, the emission band of 2Cl at a λ_{Em} of 489 nm increases while that of 2OpH at a λ_{Em} of 660 nm decreases with a raise in temperature. Plots (Fig. 3, Fig. S5 and S7, ESI‡) of the corresponding emission intensities against temperature show linear correlations in both instances with a monotonic increase in their ratio.

The ratiometric response of 2 can be exploited to probe temperature with spatial resolution at the micrometer level. Specifically, the resolved emissions of the two equilibrating species can be collected in separate detection channels of the same fluorescence microscope to allow ratiometric temperature measurements within microscaled regions of a given sample of interest. For example, 2 can be introduced within beads of alginate hydrogels. The presence of water in the beads encourages the partial

conversion of 2Cl into 2OpH to establish an equilibrium between the two species. Consistently, emission spectra (Fig. S10) of a single bead suspended in water revel the resolved bands of the two emissive species. Once again, the band of 2Cl increases and that of 2OpH decreases with a raise in the temperature of the sample. No spectral changes (Fig. S11) are instead detected if the bead is maintained at a constant temperature, indicating that the two interconverting species are stable under these conditions. Images (A, C, E and G in Fig. 4) of the bead, recorded by collecting fluorescence between 450 and 600 nm where only 2Cl emits, show an increase in emission intensity with temperature. Images (B, D, F and H in Fig. 4) of the very same sample, acquired with a detection window ranging from 600 to 770 nm where only 2OpH emits, reveal a concomitant fluorescence decrease. Indeed, the ratio (black bars in Fig. 4) between the emission intensities (yellow and purple bars in Fig. 4), integrated across the fields of view of the two channels, clearly increases with the temperature of the sample.
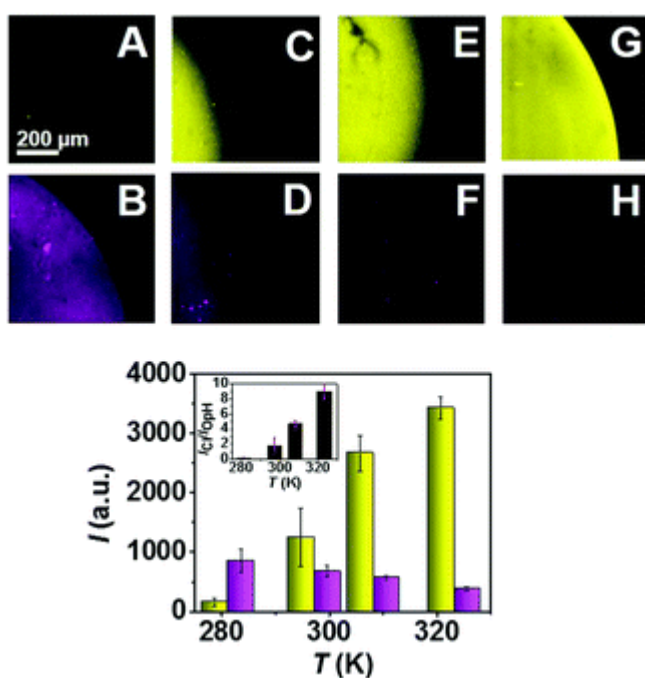

Fig. 4 Fluorescence images of an alginate bead (diameter = 1.6 mm), doped with 2 and maintained

at 281 (A and B), 297 (C and D), 308 (E and F) or 323 K (G and H) together with the corresponding emission intensities, integrated across the field of view, and their ratio (inset) [yellow channel: $\lambda_{Ex} = 405$ nm, $\lambda_{Em} = 450$–600 nm; purple channel: $\lambda_{Ex} = 561$ nm, $\lambda_{Em} = 600$–770 nm].

In summary, the equilibration of two interconverting species with resolved fluorescence results in a ratiometric response to temperature. The opening and closing of either an oxazine or an oxazolidine heterocycle are responsible for this behavior. Indeed, these structural changes affect the electronic structure of either a carbazole or a coumarin fluorophore and control the spectral position of its absorption and emission bands. In turn, the resolved emissions of the two interconverting species can be probed in parallel spectroscopically as well as measured in independent detection channels of a single microscope. In both instances, the ratio between the detected intensities can be exploited to overcome concentration effects and optical artifacts, which complicate conventional single-wavelength measurements instead. In fact, this structural design for ratiometric sensing allows the convenient mapping of temperature distributions in microscaled samples with the acquisition of conventional fluorescence images.

Conflicts of interest

There are no conflicts to declare.

Notes and references

1. J. Qiao, X. Y. Mu and L. Qi, *Biosens. Bioelectron.*, 2016, 85, 403–413
2. T. T. Bai and N. Gu, *Small*, 2016, 12, 4590–4610

3. S. Uchiyama, C. Gota, T. Tsuji and N. Inada, *Chem. Commun.*, 2017, 53, 10976–10992 .

4. H. Y. Zhou, M. Sharma, O. Berezin, D. Zuckerman and M. Y. Berezin, *ChemPhysChem*, 2016, 17, 27–36.

5. B. del Rosal, E. Ximendes, U. Rocha and D. Jaque, *Adv. Opt. Mater.*, 2017, 5, 1600508

6. M. Quintanilla and L. M. Liz-Marzan, *Nano Today*, 2018, 19, 126–145

7. J. R. Lakowicz, *Principles of Fluorescence Spectroscopy*, Springer, New York, 2006

8. S. Uchiyama, A. P. de Silva and K. Iwai, *J. Chem. Educ.*, 2006, 83, 720–727

9. C. Pietsch, U. S. Schubert and R. Hoogenboom, *Chem. Commun.*, 2011, 47, 8750–

10. X.-D. Wang, O. S. Wolfbeis and R. J. Meier, *Chem. Soc. Rev.*, 2013, 42, 7834–7869

11. J. Rocha, C. D. S. Brites and L. D. Carlos, *Chem. – Eur. J.*, 2016, 22, 14782–14795

12. T. Y. Qin, B. Liu, K. N. Zhu, Z. J. Luo, Y. Y. Huang, C. J. Pan and L. Wang, *TrAC, Trends Anal. Chem.*, 2018, 102, 259–271

13. E. J. McLaurin, L. R. Bradshaw and D. R. Gamelin, *Chem. Mater.*, 2013, 25, 1283–

14. S. Uchiyama and C. Gota, *Rev. Anal. Chem.*, 2017, 36,

15. Y. Cheng, Y. Gao, H. Lin, F. Huang and Y. S. Wang, *J. Mater. Chem. C*, 2018, 6, 7462–7478

16. T. Barilero, T. Le Saux, C. Gosse and L. Jullien, *Anal. Chem.*, 2009, 81, 7988–8000

17. X. D. Wang, X. H. Song, C. Y. He, C. J. Yang, G. Chen and X. Chen, *Anal. Chem.*, 2011, 83, 2434–2437

18. T. Liu and S. Y. Liu, *Anal. Chem.*, 2011, 83, 2775–2785

19. T. Kan, H. Aoki, N. Binh-Khiem, K. Matsumoto and I. Shimoyama, *Sensors*, 2013, 13, 4138–4145

20. J. Liu, X. Guo, R. Hu, J. Xu, S. Wang, S. Li, Y. Li and G. Yang, *Anal. Chem.*, 2015, 87, 3694

21. *Organic Photochromic and Thermochromic Compounds*, ed. J. C. Crano and R. Guglielmetti, Plenum Press, New York, 1999

22. M. Tomasulo, S. Sortino and F. M. Raymo, *J. Photochem. Photobiol., A*, 2008, 200, 44–49

23. E. Deniz, M. Tomasulo, J. Cusido, S. Sortino and F. M. Raymo, *Langmuir*, 2011, 27, 11773–11783

24. Y. Zhang, S. Tang, E. R. Thapaliya, L. Sansalone and F. M. Raymo, *Chem. Commun.*, 2018, 54, 8799–8809

25. E. Deniz, M. Tomasulo, J. Cusido, I. Yildiz, M. Petriella, M. L. Bossi, S. Sortino and F. M. Raymo, *J. Phys. Chem. C*, 2012, 116, 6058–6068

26. J. Cusido, S. Shaban Ragab, E. R. Thapaliya, S. Swaminathan, J. Garcia-Amorós, M. J. Roberti, B. Araoz, M. M. A. Mazza, S. Yamazaki, A. M. Scott, F. M. Raymo and M. L. Bossi, *J. Phys. Chem. C*, 2016, 120, 12860–12870

27. J. Garcia-Amorós, S. Swaminathan, S. Sortino and F. M. Raymo, *Chem. – Eur. J.*, 2014, 20, 10276–10284

28. Q. H. You, Y. M. Lee, W. H. Chan, N. K. Mak, A. W. Lee, S. C. Hau and T. C. Mak, *RSC Adv.*, 2015, 5, 4099–4102

29. R. G. Parr and W. Yang, *Density-Functional Theory of Atoms and Molecules*, Oxford University Press, Oxford, 1989

30. F. M. Raymo, *J. Phys. Chem. A*, 2012, 116, 11888–

31. D. R. Lide, *CRC Handbook of Chemistry and Physics*, CRC Press, Boca Raton, 2011

32. G. J. Kavarnos, *Fundamentals of Photoinduced Electron Transfer*, VCH, New York, 1993